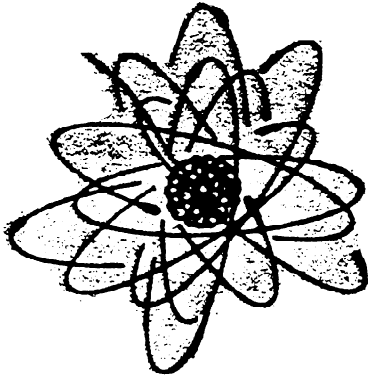


**W. H. ARNOLD, JR., "CRITICAL MASSES AND LATTICE PARAMETERS OF H₂O-
UO₂, CRITICAL EXPERIMENTS. A COMPARISON OF THEORY AND
EXPERIMENT," WESTINGHOUSE ATOMIC POWER DEPARTMENT REPORT
YAEC-152 (NOVEMBER 1959).**

YAEC - 152



YANKEE ATOMIC ELECTRIC COMPANY
RESEARCH AND DEVELOPMENT PROGRAM

CRITICAL MASSES AND LATTICE
PARAMETERS OF $H_2O - UO_2$ CRITICAL
EXPERIMENTS: A COMPARISON OF
THEORY AND EXPERIMENT

R & D SUBCONTRACT NO.1 UNDER
USAEC-YAEC CONTRACT AT(30-3)-222

NOVEMBER 1959

WESTINGHOUSE ELECTRIC CORPORATION
ATOMIC POWER DEPARTMENT
PITTSBURGH,30 P. O. BOX 355 PENNSYLVANIA

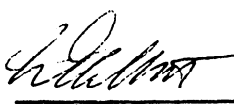


YANKEE ATOMIC ELECTRIC COMPANY
RESEARCH AND DEVELOPMENT PROGRAM

CRITICAL MASSES AND LATTICE PARAMETERS
OF H_2O-UO_2 CRITICAL EXPERIMENTS:
A COMPARISON OF THEORY AND EXPERIMENT

W. H. Arnold, Jr.
Reactor Development
Reactor Physics Design Section

NOVEMBER 1959

APPROVED: 
W. E. Abbott, Mgr.
Reactor Development

WARRANTY

The Westinghouse Electric Corporation, Government Agencies, Prime Contractors, Sub-Contractors, or their Representatives or other agencies make no representation or warranty as to the accuracy or usefulness of the information or statements contained in this report, or that the use of any information, apparatus, method or process disclosed in this report may not infringe privately-owned rights. No assumption of liability is assumed with respect to the use of, or for damages resulting from the use of, any information, apparatus, method or process disclosed in this report.

Westinghouse
ELECTRIC CORPORATION
ATOMIC POWER DEPARTMENT
P.O. BOX 355
PITTSBURGH 30, PA.

TABLE OF CONTENTS

	<u>PAGE</u>
ABSTRACT	3
LIST OF FIGURES.	4
LIST OF TABLES	4
LIST OF SYMBOLS.	5
I. INTRODUCTION.	7
II. A SEMI-EMPIRICAL THEORY OF REACTOR STATICS.	13
1. The Neutron Cycle Model.	13
2. η_f and P_{NL2}	15
3. ϵ	17
4. P_{NL1} and P_{NL2}	18
5. p_{28}^U and p_{28}^L	19
6. p_{25} and η_{25}^R	21
7. p_c	21
III. H ₂ O-UO ₂ CRITICAL EXPERIMENT DATA.	24
IV. COMPARISON BETWEEN EXPERIMENT AND THE SEMI-EMPIRICAL THEORY	28
1. Quantities which are independent of a and b.	28
2. Fitting of a and b.	28
V. A SYSTEM INVOLVING THE MUFT CODE AND ITS COMPARISON WITH EXPERIMENT.	33
APPENDIX A GROUP CONSTANTS AND k_{eff}	36
APPENDIX B FAST FISSION CONSTANTS.	39
APPENDIX C U-238 RESONANCE CONSTANTS	41
APPENDIX D U-235 RESONANCE CONSTANTS	42
APPENDIX E MODIFICATION OF MUFT CODE	44
REFERENCES	45
ACKNOWLEDGEMENTS	47

ABSTRACT

This report describes a semi-empirical method of performing lattice calculations in $\text{UO}_2\text{-H}_2\text{O}$ cores which was developed under the Yankee Research and Development Program, and which has been used in the design of Yankee core 1. Calculated results using this method give close agreement with experimental results, presented here, from the Westinghouse Bettis TRX facilities, from the Yankee and BR-3 critical experiments performed at the Westinghouse Atomic Power Department, and from a critical experiment performed by Babcock and Wilcox for the NSS Savannah.

Although the semi-empirical method gives adequate agreement, another system of calculation is presented which uses the MUFT code and has a somewhat firmer theoretical justification. It should prove valuable in the design of future cores.

LIST OF FIGURES

FIGURE NUMBER		<u>PAGE</u>
1	The Neutron Life Cycle	14
2	U-235 Homogeneous Resonance Integral and λ_R Versus Dilution	22
3	Contour Plot to Determine Best Fit of a and b	32

LIST OF TABLES

TABLE NUMBER		<u>PAGE</u>
1	Candle Group 1 Cross Sections	18
2	One Group Cross Sections for τ Calculation	19
3	Resonance Neutron Constants	20
4	Capture Integrals	23
5	UO ₂ -H ₂ O Experimental Data	25
6	Physical Data of Experimental Lattices	26
7	Homogenized Number Densities in Experimental Lattices	27
8	Hand Calculated Lattice Parameters Independent of a and b	29
9	Fit of k (using B_{crit}^2) as a Function of a and b	30
10	Comparison of Experiment with Semi-Empirical Model	31
11	Use of MUFT Code in Comparison with Experiment	35
A1	Comparison Between k_2 , k_4 , and WANDA Eigenvalues	38
A2	U-235 Resonance Parameters	43

LIST OF SYMBOLS

(NOTE: Many of the symbols below are used with subscripts 25 and 28, which refer to U-235 and U-238, respectively.)

$\frac{R}{\lambda_{25}}$	Ratio of capture to fission in U-235 above 0.625 ev.
β	A reactivity multiplication factor for U-235 resonance fissions.
$\Gamma, \text{ ev}$	Channel width in Breit-Wigner formula. Subscript f refers to probability of fission, γ , to radiative capture.
δ_{28}	Ratio of U-238 fissions to U-235 fissions.
δ_{25}	Ratio of U-235 fissions above 0.625 ev to those below 0.625 e
$\bar{\delta}_{28}$	Value of δ_{28} when leakage and fast capture are ignored.
ϵ	Fast neutron multiplication factor.
η	Number of neutrons released per neutron absorbed by fuel.
η_{25}^R	Number of neutrons released per neutron of energy above 0.625 ev absorbed by U-235.
η_f	Number of fission neutrons released per thermal neutron absorbed.
ν	Number of neutrons released per fission.
ξ	Average lethargy gain per collision.
ρ_{28}	Ratio of U-238 captures above 0.625 ev to those below 0.625.
$\partial\rho/\partial B^2, \text{ cm}^2$	Rate of change of reactivity with change in core buckling.
$\Sigma, \text{ cm}^{-1}$	Macroscopic cross section. Numerical subscripts indicate group number, counting from 1 as the highest energy group. (s and f also refer to slow and fast groups in a 2 group scheme.) Letter subscripts are: a = absorption, f = fission, c = nonfission absorption, s = scattering, tr = transport, r = removal, sl = slowing down.
$\sigma, \text{ barn}$	Microscopic cross section. See Σ for an explanation of subscripts used.
$\sigma_{amax}, \text{ barn}$	Peak absorption cross section of a Breit-Wigner resonance.

LIST OF SYMBOLS CONT'D

τ , cm ²	Fast migration area.
$\bar{\phi}_3 / \bar{\phi}_1$	Disadvantage factor: ratio of average thermal flux in moderator to average thermal flux in fuel.
χ_i	The fraction of fission neutrons which appear in group i.
a, b	Two empirically fitted constants. See text, Section II, 1.
B^2 , cm ⁻²	Buckling.
D, cm	Diffusion coefficient. See definition of Σ for an explanation of subscripts.
E_0 , ev	Energy of a resonance.
f	Thermal utilization.
k_{eff} , k	These symbols have been used to designate a number which answers the question: "By what number must ν be divided in order that the neutron flux have zero time derivative."
L	Resonance self-shielding factor used in MUFT.
L^2 , cm ²	Thermal diffusion area.
p	Resonance escape probability.
P_{28}^U	That part of the U-238 resonance escape probability which is designated (artificially) to lie above U-235 resonances.
P_{28}^L	That part of the U-238 resonance escape probability which is designated to lie below U-235 resonances.
P_c	Capture escape probability of neutrons above 0.625 ev for materials other than U-235 and U-238.
P_{NL}	Non-leakage probability, $P_{NL} = P_{NL1} P_{NL2} P_{NL3}$. Subscript 1 refers to the range from fission to U-235 resonances; 2, to the range from 25 resonances to thermal; while P_{NL3} is the thermal non-leakage probability.
R	Escape probability for control material, $R = R_s R_f$. R_f refers to neutrons above 0.625 ev, while R_s refers to the range below 0.625 ev.
RI, barn	Resonance integral.

I. INTRODUCTION

In the present status of the design of large pressurized water power reactors, the uncertainties attendant to the calculation of reactivity can be extremely expensive in terms of the additional equipment or design restrictions required to cover them. If we consider a plant such as Yankee, in which the control rods are required to shut the core down to a k_{eff} of .97 in the hot, clean, zero power condition; the expense of the reactivity uncertainty will manifest itself either in the purchase of extra control rods and mechanisms (or shims) or in the specification of a lower enrichment, and hence shorter core life, than might otherwise have been possible. The price tags which one can attach to various degrees of uncertainty are sufficiently large that one can afford to spend considerable sums on reactor experiments and the analysis of data from such experiments. This report and a companion, YAEC-62¹, discuss the analysis of a series of experiments performed by the Westinghouse Reactor Evaluation Center on part-core mock-ups of the Yankee Reactor, described in YAEC-94². The Yankee Reactor has a particularly clean mechanical design so that the lattice experiments performed should have general interest for workers in this field.

Returning to the subject of reactivity calculations, let us examine the various stages reached during life in a reactor to show where uncertainties appear and at which points the experiments have proven valuable.

1. Cold clean core. Here the important quantities involve such things as the fast effect in U-238; resonance capture in U-238, U-235, structural material, and oxygen; thermal neutron cross sections, disadvantage factors, and spectra; and neutron slowing down and leakage in the presence of these other effects. These will be the major concern of this report, as the critical experiments discussed are of the cold, clean type. In the Yankee reactor it is not necessary to be

overly concerned with the value of the cold clean k_{eff} because the soluble chemical shutdown system is elastic enough to cover any conceivable uncertainty in calculation.

2. Hot clean core at zero power. This k_{eff} is the important number for initial shutdown as the control rods alone must shut down the core by 3%. Thus, with a given amount of control surface^{*}; one must set the initial enrichment at a value such that, even in the face of an adverse combination of uncertainties in the calculation of the unrodded k_{eff} and the rod worths, the desired shutdown multiplication is reached.

The calculation of rod worths based on a portion of the critical experiment data has been discussed in YAEC-62. No experiments have been performed which would bear directly on the hot, clean unrodded k_{eff} because these would have required a pressurized critical assembly. Thus we are forced to rely on extrapolation from cold clean critical experiments.

There are four major effects entering into the cold to hot reactivity swing of a reactor; the change in neutron temperature, Doppler broadening of resonances, a change in the scale factors (because of the density change) of fast neutron slowing down and diffusion in water compared to the other elements present, and the change in the ratio of fuel and water number densities (also because of density changes). The last of these effects is covered by performing the cold critical experiments at several volume ratios of H_2O/U . The remaining three must be calculated on the basis of less direct evidence.

* 24 control rods are provided in the first Yankee core; in addition, there is the possible, but undesirable, use of eight poison shims - see reference 1.

3. Hot core at end of life under equilibrium poisoning at full power. In the Yankee first core the multiplication factor corresponding to this core condition is by definition unity. In other words, the life of the core is a dependent variable once the enrichment has been fixed to conform to a given amount of control surface. Were a core to be designed with a fixed lifetime in mind then one would have to work backwards from an end of life multiplication, enough greater than one to allow for uncertainties, to an initial enrichment. In this case the control surface must be the dependent variable and the compounding of uncertainties would reflect itself in increases in rod surface requirements.

In the interests of completeness it is well to mention the factors which make the calculation of multiplication factors of reactors which have been operated for some time different from hot clean cores: cross sections of U, Pu, and other heavy elements which build up; complications of neutron spectra due to the low-lying resonances of these heavy elements; the non-uniform buildup of Pu isotopes in individual fuel rods because of surface resonance absorption by U-238 and thermal neutron distributions which also peak towards the surface; Doppler broadening of resonances the difficulty of whose calculation is compounded by the tremendous range of UO_2 temperatures in a given pellet; the cross section behavior of the numerous fission products and their buildup, decay, and transformation; and the "hysteresis" effect of control rod programming which makes the control position and power shape at a given moment depend on the entire previous history of the reactor.

Reliable design information on the reactivity at these various stages in a $\text{UO}_2\text{-H}_2\text{O}$ core will not be available until a number of reactors have run through their lives. In the meantime we are forced to rely on calculations and accept the attendant uncertainties. Wherever these calculations can be subjected to experimental tests, we must seize the opportunity to improve them. Thus the author feels that the design of reactor experiments should be undertaken with a view to providing the severest possible tests of theory. This often conflicts with the viewpoint of many who would perform experiments only within the "design range" of the various reactor variables.

Having set the stage with these generalities of reactor physics design, let us narrow our field of view to cold, clean critical experiments and their use to improve the methods applied to reactor design. The critical experiment data used was expanded to include all available information on $\text{H}_2\text{O-UO}_2$ systems, described in Section III below. This decision to employ data other than that obtained under the Yankee R and D Program is justified by the necessity of providing the severest possible test of theory. Indeed it would be indefensible to restrict one's view to the Yankee experiments alone and proceed to the design of multi-million dollar reactors.

The theories employed by reactor physicists are almost as numerous as reactor physicists, but they can be separated into two general classifications. The first of these might be called the microscopic approach. One starts with basic cross section data on the interactions between neutrons and nuclei. Then he builds up descriptions of reactors by using this data in Monte Carlo calculations or in the Boltzmann equation, a fundamental relation allowing statistical distributions of neutrons to be calculated. This approach is extremely satisfying on theoretical grounds, but is difficult to carry out because of gaps and uncertainties in the cross section data; and because of computational difficulties involved in solving the Boltzmann equation, or performing the Monte Carlo calculations. It seems inevitable that this "pure" approach will come into greater favor as experiments continue to refine

and fill gaps in the cross section data, and as digital computers allow the performance of previously unthinkable calculations.

The other approach might be called the macroscopic one. This is the familiar one involving the semi-empirical quantities such as p , ϵ , f , τ , etc. Of course it too makes use of cross section data but the main reliance is on integral experiments to provide empirical fits which reduce a function of a vast number of variables to an approximate dependence on a very few parameters, valid within a known range of variation. This approach was the only one possible before the advent of detailed cross section information and large digital computers. It is likely to be perpetuated by the need to employ it in studies which require broad surveys to be performed by relatively simple and quick hand calculations.

Section II below is concerned with such a semi-empirical approach which seems to do remarkably well over the range of critical experiments described in Section III. It was devised to include all effects known to have a major effect on reactivity leaving two parameters to be adjusted to achieve the best experimental fit. It was necessary to employ this approach because the microscopic one was not sufficiently developed to allow its use in the design of the Yankee first core*.

The use of the microscopic approach does give the designer greater confidence when he must extrapolate beyond the range of variables covered by his experimental information. A later section of this report describes a calculation scheme which relies much more heavily on the microscopic data, and which may have potential for future use in low enrichment pressurized water reactor design.

* At this time it was possible to employ a more or less "pure" approach in the design of highly enriched reactors. The problem of heterogeneous resonance capture in low enrichment uranium was the main deterrent to the use of such a scheme in Yankee.

The basic problem in calculating the low enrichment, H₂O moderated system seems to have been the failure in principle of any model which attempts to separate three effects which occur simultaneously to as many as 50% of all neutrons slowing down through the energy band from a few ev to a few thousand, namely; leakage, resonance capture in U-238, and resonance capture and fissions in U-235. A number of attempts to reconstruct the rates of these processes from measurements or calculations of each one in the absence of the other two have failed, seemingly because of interactions among the three. A solution of this problem has been the major aim of the work presented below.

II. A SEMI-EMPIRICAL THEORY OF REACTOR STATICS

1. The Neutron Cycle Model

Figure 1 is a schematic diagram of a neutron life cycle. It involves a feedback term due to U-235 resonance fissions which are neither fast nor thermal. (The similar U-238 fast fission term need not be represented explicitly in terms of feedback because no other processes are assumed to be interposed between the neutrons causing these fissions and the ones resulting.)

To derive an algebraic formula for k_{eff} from Figure 1, consider one thermal neutron absorbed at (A); ηf neutrons will reach (B). If x is temporarily assumed to be the number that reach (B) due to epithermal fissions, then $(\eta f + x) \epsilon$ neutrons reach (C), and $(\eta f + x) \epsilon P_{NL1}^U P_{28}^U$ reach (D). Thus we are able to construct a relationship which can be solved for x :

$$x = \eta_{25}^R (1 - p_{25}) \left[(\eta f + x) \epsilon P_{NL1}^U P_{28}^U \right] \quad (1)$$

from which:

$$\eta f + x = \eta f \left[1 - \eta_{25}^R \epsilon P_{NL1}^U P_{28}^U (1 - p_{25}) \right]^{-1} \cdot \epsilon \quad (2)$$

To continue around the loop, $(\eta f + x) \epsilon P_{NL1}^U P_{28}^U P_{25}^L P_{28}^L p_c R_F P_{NL2}$ reach (E), and the number reaching (A) again is: $(\eta f + x)$.

$$k_{eff} = \frac{R_F P_{NL1} P_{NL2} P_{NL3} \eta f \epsilon p_c P_{28}^U P_{28}^L \beta}{S - F} \quad (3)$$

where

$$\beta = \frac{P_{25}}{1 - \epsilon P_{NL1}^U P_{28}^U \eta_{25}^R (1 - p_{25})}$$

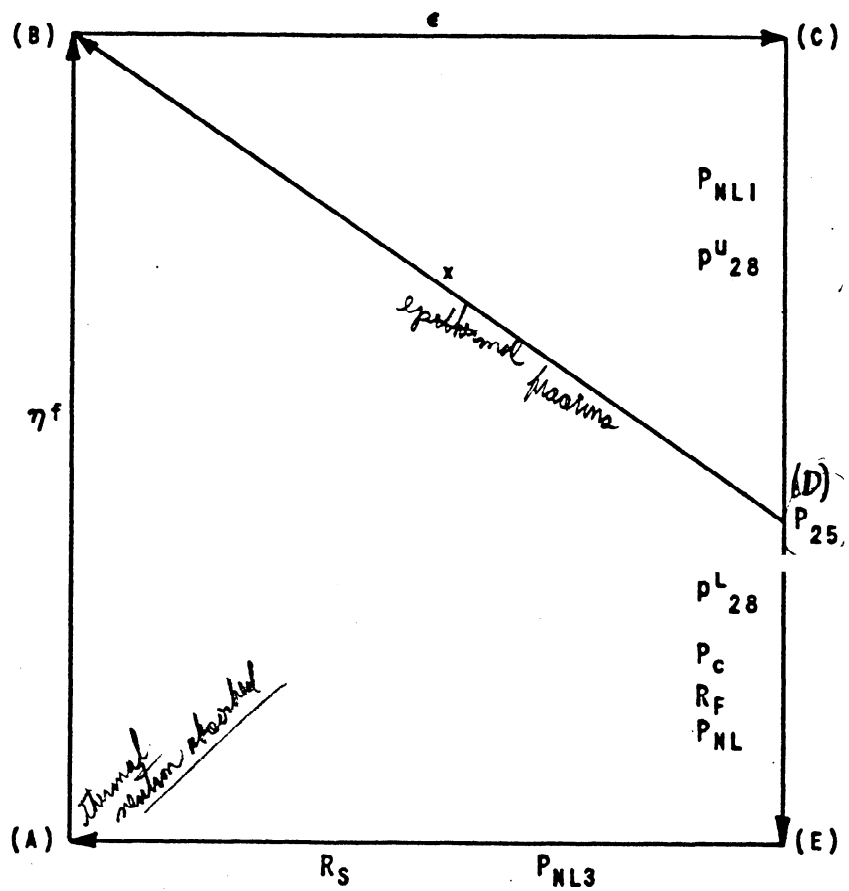


FIGURE I
THE NEUTRON LIFE CYCLE

This is felt to be about the simplest model which contains a treatment of all important effects. The key to the scheme lies in the quantities P_{NL1} and P_{NL2} , and p_{28}^U and p_{28}^L . The product of the first pair is what is normally called the fast nonleakage probability, while the second pair are factors of the usual p_{28} . They have been split to allow an empirical fit to account for the complex interactions between leakage, U-238 resonance captures, and U-235 resonance fission feedback. The two fittable parameters of the scheme express the position at which artificial cuts are made in fast leakage and U-238 resonance capture.

It is important to note that the bleedoff of neutrons at p_{25} implies that the rate of resonance captures in U-238 is not calculable from the simple product $p_{28}^U p_{28}^L$, nor is the rate of fast neutron leakage obtained from $P_{NL1} P_{NL2}$. Thus the $p_{28} = p_{28}^U p_{28}^L$ used in this scheme is a fictitious quantity intended to apply to a reactor without U-235; a similar remark applies to fast leakage. The remainder of this section is devoted to describing the calculation of the factors appearing in the neutron cycle. R_S and R_F are discussed in reference 1 and will not be further described here.

2. η_f and P_{NL2}

The quantity η_f (the number of fission neutrons released per thermal neutron absorbed) is calculated in two stages. First, flux ratios in the unit cell are calculated using unhardened Maxwellian constants in the method of Amouyal and Benoist^{3,4}. The important number here is $\bar{\phi}_3 / \bar{\phi}_1$, the ratio between average moderator flux and the average flux in the fuel; the clad flux is arbitrarily assumed to lie halfway between. Then these flux factors are used to obtain flux weighted material number densities which then form the input to a run of the SOFOCATE⁵ Wigner-Wilkins flux spectrum code. This code finds the hardened spectrum (including the 1/E part) to 0.625 ev, on a hydrogen gas moderation model, and averages cross section data over this spectrum to find averaged microscopic cross sections and the

macroscopic thermal neutron group constants $\nu\Sigma_f$, Σ_a , and D_s . Then, ηf is the ratio of $\nu\Sigma_f$ to Σ_a , while L^2 is D_s over Σ_a . We assume P_{NL3} to be $(1 + L^2 B^2)^{-1}$.

It is important to note the absolute cutoff at 0.625 ev. This means that all $1/v$ absorption above this value must be included in p_c , p_{28}^L , or p_{25} . It is difficult to justify any particular value of this cutoff, except to say that it should be high enough so that no upward (in energy) scattering of neutrons should occur above it. 0.625 ev fulfills this criterion and is near, though somewhat above, the effective cutoff energy of a 20 mil cadmium foil. It is also convenient because it is normally used as the lower limit of the MUFT Code⁶.

A remark should be inserted at this point regarding the use of a hydrogen gas model. Perhaps a code based on the Wilkins model (infinite scatter mass) would be more appropriate, as chemical binding of the H_2O molecule gives scattering by hydrogen the effect of scattering by an element of atomic weight somewhere between one and eighteen. In any event, it is not felt that the spectra are appreciably different provided one has the proper ratio between Σ_a and $\xi\Sigma_s$, so that SOFOCATE has been used because it was available.

Another point to be noted is that the SOFOCATE is run for an homogenized mixture of fuel and moderator, so that the assumption of identical spectra in the two regions is implicit. Because of the small size of the unit cell, this is not felt to be too important an effect. In any event the method of measurement of the unit cell flux ratio, with which the calculated values are in excellent agreement, makes the same assumption.

3. $\underline{\epsilon}$

We define ϵ to be the ratio of the net number of fission neutrons formed with U-235 and U-238 fissions to the number without U-238 fissions, in a fictitious reactor where there is no leakage or radiative capture down to 0.81 Mev. This rather involved definition seems, and is, quite arbitrary; but the effects thus ignored in ϵ are included in the other factors introduced below. The cutoff of 0.81 Mev is also arbitrary; it is near the cutoff energy of the fission cross section in U-238, and is convenient because it is the usual choice of the cut between groups one and two in the MUFT-CANDLE four group scheme. One can then use CANDLE group 1 fitted constants to calculate ϵ .

The formula for ϵ is conveniently derived via the quantity δ_{28} , the ratio of U-238 fissions to all other fissions. When performing experimental lattice studies in detail, one generally measures δ_{28} . As shown in Appendix B, this can be written:

$$\delta_{28} = \frac{\nu_{25}}{\nu_{28}} \left[\frac{\chi_1 \nu \Sigma_{1f28}}{D_1 B^2 + \Sigma_{1a} + \Sigma_{1r} - \chi_1 \nu \Sigma_{1f28}} \right] \quad (4)$$

Before proceeding to ϵ , we must introduce another quantity, $\bar{\delta}_{28}$, which applies to the fictitious reactor which has $B^2 = 0$ and $\Sigma_{1a} = \Sigma_{1f28}$. Then ϵ is obtained from a simple neutron balance:

$$\epsilon = 1 + \bar{\delta}_{28} \left(\frac{\nu_{28} - 1}{\nu_{25}} \right) \quad (5)$$

$$= \frac{\Sigma_{1r} + (1 - \chi_1) \Sigma_{1f28}}{\Sigma_{1r} - (\chi_1 \nu_{28} - 1) \Sigma_{1f28}} \quad (6)$$

Table 1 contains the CANDLE fitted constants used in the calculation of ϵ and δ_{28} . These constants were fitted by R. G. St. Paul to a number of MUFT runs on cores of compositions similar to those described in these critical experiments.

TABLE 1

CANDLE Group 1 Cross Sections

<u>Nuclide</u>	<u>σ_{f1}</u>	<u>σ_{a1}</u>	<u>σ_{tr1}</u>	<u>σ_{r1}</u>
H	0	0	1.54	1.48
O	0	0.0338	1.42	0.268
Al	0	0.0089	2.02	0.334
Fe or SS	0	0.0023	2.38	0.431
25	1.300	1.437	6.59	2.21
28	0.418	0.470	5.73	2.21

$$\chi_1 = .75165;$$

$$\nu_{28} = 2.66$$

4. P_{NL1} and P_{NL2}

These quantities are derived from a one fast group slowing down model, in which the product $P_{NL1} P_{NL2}$ is taken to be $(1 + \tau B^2)^{-1}$. The split between P_{NL1} and P_{NL2} is expressed by the fittable constant b:

$$P_{NL1} = \frac{1}{1 + b \tau B^2} \quad (7)$$

An estimate of b can be made by noting that about 0.8 of the lethargy between fission and thermal energies lies above the resonance band in U-235.

The neutron age, τ , is calculated from a one velocity fit to various measured ages in elements and simple mixtures, which yield the one fast group cross sections of Table 2.

$$\tau = \frac{1}{3 \Sigma_{trf} \Sigma_{sl}} \quad (8)$$

TABLE 2

One Group Cross Sections for τ Calculation

Nuclide	σ_{trf}	σ_{sf}
H	1.85	0.655
O	3.31	0.027
Al	2.25	0.012
Fe or SS	4.38	0.064
U	9.00	0.800

The τ of a reactor lattice is generally not directly measurable. Instead, one normally makes experimental measurements of the change in reactivity per unit change in B^2 by the partial water height or poison methods. A prediction of the expected result can be made by differentiating equation 3 (after making the substitutions $P_{NL1} = (1 + b \tau B^2)^{-1}$, $P_{NL2} = (1 + \tau B^2)^{-1}$, $P_{NL3} = (1 + L^2 B^2)^{-1}$).

$$\frac{1}{k} \frac{\partial k}{\partial B^2} = - \frac{\tau}{1 + \tau B^2} - \frac{L^2}{1 + L^2 B^2} - \frac{b \tau}{1 + b \tau B^2 - A} + \frac{b \tau}{1 + b \tau B^2} \quad (9)$$

$$A \equiv \eta_{25}^R \epsilon p_{28}^U (1 - p_{25}) \quad (10)$$

5. p_{28}^U and p_{28}^L

The product of these two quantities, called p_{28} is computed from Hellstrand's measured resonance integral⁷ (to which a $1/v$ term has been added):

$$p_{28}^U p_{28}^L = p_{28} = \exp \left[- \frac{N_{28}}{\xi \Sigma_s} (5.23 + 26.5 D \sqrt{\frac{S}{M}}) \right] \quad (11)$$

$\xi\Sigma_s$ is calculated from the microscopic constants of Table 3. D is a Dancoff correction⁸, which has been modified by French⁹ to account for the incomplete shielding of small UO₂ rods which cannot be said to be completely black to resonance neutrons. S/M is the usual ratio of fuel surface to UO₂ mass.

The split between p_{28}^U and p_{28}^L is made via the second fittable constant, a:

$$p_{28}^U = (p_{28})^a \quad ; \quad p_{28}^L = (p_{28})^{1-a} \quad (12)$$

There is another quantity related to p_{28} which is more easily measurable in a reactor lattice. This is ρ_{28} , defined via the ratio between the activities of a properly shaped U-238 foil with and without a cadmium cover. As shown in Appendix C, this can be written as:

$$\rho_{28} = P_{NL1} \epsilon \frac{\eta f}{F_{28}} \beta \left[1 - p_{28}^U + p_{28}^U p_{25} - p_{25} p_{28} \right] \quad (13)$$

A consideration of the reaction rate as calculated from equation (13) will show that p_{28} alone would give the correct rate only in an equivalent reactor without leakage or U-235 fission. Thus equation (13) exhibits most clearly the interaction between resonance captures, resonance fissions, and leakage during the slowing down process. (p_{28} is, therefore, a fictitious quantity in much the same sense as ϵ .)

TABLE 3
Resonance Neutron Constants

<u>Nuclide</u>	<u>σ_s</u>	<u>$\xi\sigma_s$</u>
H	20.1	20.1
O	3.8	0.460
Al	1.4	0.100
Fe or SS	12.0	0.420
U	9.5	0.080

6. p_{25} and η_{25}^R

These are calculated from a homogeneous model, from capture and fission resonance integrals which have been calculated from published resonance parameters (plus $1/v$ contributions) as a function of dilution to include energy self-shielding. Figure 2 is a plot of RI_{25} and χ_{25}^R as functions of Σ_s/N_{25} , the scattering cross section per U-235 atom. A description of the calculations leading to this figure is presented in Appendix D. One then calculates p_{25} and η_{25}^R as follows:

$$p_{25} = \exp \left[- \frac{N_{25}}{\xi \Sigma_s} RI_{25} \right] \quad (14)$$

$$\eta_{25}^R = \frac{2.47}{1 + \chi_{25}^R} \quad (15)$$

As is the case with the other factors, neither p_{25} nor η_{25}^R are measured in lattice experiments. By comparing the fission product activities of fuel wrapped in Cd foil with fuel not so wrapped, one derives δ_{25} , the ratio of U-235 nonthermal fissions to U-235 thermal fissions. In a derivation quite similar to the method by which equation (13) was obtained, the model of Figure 1 yields:

$$\delta_{25} = \frac{\beta}{p_{25}} - 1 \quad (16)$$

7. p_c

This factor is calculated, using a homogeneous model, from the set of infinite dilution capture integrals (including $1/v$ terms) presented in Table 4.

$$p_c = \exp \left[- \frac{\sum_i N_i RI_i}{\xi \Sigma_s} \right] \quad (17)$$

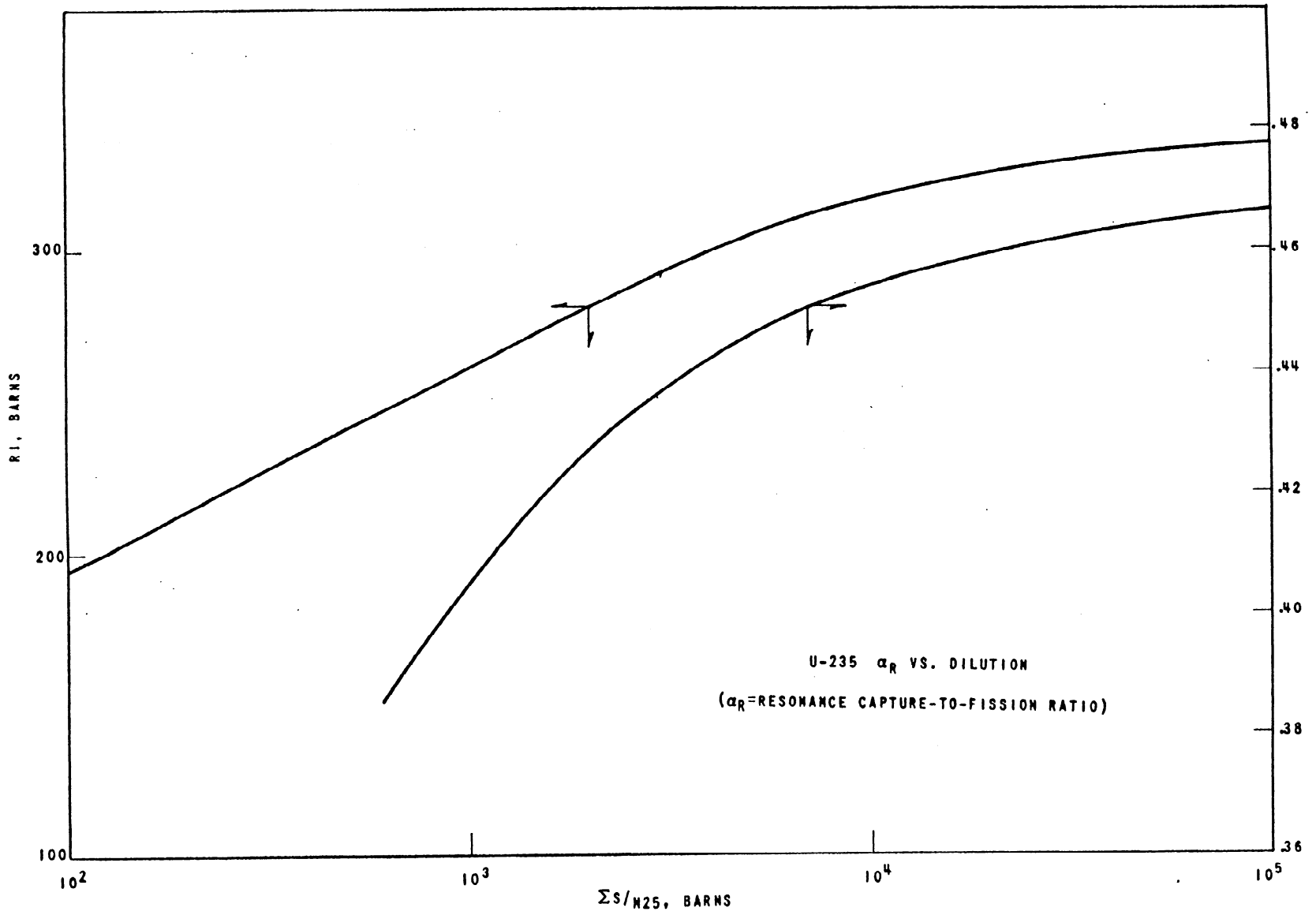


FIGURE 2
U-235 HOMOGENEOUS RESONANCE INTEGRAL VERSUS DILUTION

TABLE 4

Capture Integrals

<u>Nuclide</u>	<u>RI, barns</u>
H	0.132
O	0.088
Al	0.18
304 SS	2.53
348 SS	2.65

III. H₂O-UO₂ CRITICAL EXPERIMENT DATA

The experimental data employed in this study was obtained by workers at the Westinghouse Bettis plant from the TRX lattices¹⁰, from Yankee critical experiment studies performed by the Westinghouse Atomic Power Department², from a Babcock and Wilcox Nuclear Ship Savannah critical¹⁰, and from some critical experiments performed by Westinghouse APD utilizing the fuel for a small pressurized water reactor for Belgium, the BR-3¹⁷. Some of the data for the three Yankee lattices was obtained from reference 17.

Table 5 contains the experimental information of value in checking lattice calculations, extracted from the reports describing the experiments. Table 6 gives a physical description of the lattices employed, while in Table 7 a set of homogenized material number densities is presented which was either calculated from the physical descriptions supplied by, or obtained directly from, the experimental groups.

It would be out of place in this report to attempt a critical discussion of the experimental data, so it is presented at face value except for a correction of δ_{25} and ρ_{28} to a 0.625 ev cutoff. The publications of the various experimental groups themselves should be consulted for further information on the data.

TABLE 5

UO₂-H₂O Experimental Data

Case (See Table 2)	Enrich- ment w/o 235	Boron Conct. ppm	W/U*	B ² _{crit} m ⁻²	-∂ρ/∂B ² cm ²	ρ ₃ /ρ ₁	δ ₂₅ **	δ ₂₈	ρ ₂₈
1 TRX h [†]	1.3		3	28.37	48 ± 2	1.09 ± .03	.075 ± .003 - .008	.071 ± .007	1.19 ± .04
2 TRX h	1.3		4	30.17	46 ± 2	1.14 ± .03	.072 ± .002 - .010	.059 ± .006	.994 ± .013
3 TRX h	1.3		5	29.06	41 ± 2	1.16 ± .03	.067 ± .002 - .010	.051 ± .004	.807 ± .014
4 TRX h	1.3		4	25.28	47 ± 2	1.10 ± .01	.073 ± .002 - .010	.063 ± .003	1.04 ± .05
5 TRX h	1.3		5	25.21	48 ± 2	1.10 ± .01	.053 ± .002 - .009	.054 ± .003	.901 ± .02
6 TRX h	1.3		3	32.59	41 ± 2	1.10 ± .01	.088 ± .002	.078 ± .004	1.43 ± .01
7 TRX h	1.3		4	35.47	39 ± 2	1.13 ± .01	.067 ± .001	.070 ± .004	1.15 ± .01
8 TRX h	1.3		5	34.22	36 ± 2	1.13 ± .01	.052 ± .001	.057 ± .003	.934 ± .01
9 YPR S	2.7		2.2	40.75	38 - 43				2.77 ± .08
9A YPR S	2.7	439	2.2	28.9					
10 YPR S	2.7		2.9	53.23	37 - 38	1.16 ± .05	.15 ± .01	.076 ± .002	2.22 ± .05
10A YPR S	2.7	739	2.9	26.9					
11 YPR S	2.7		3.9	63.26	32 - 36	1.16 ± .03		.060 ± .005	1.85 ± .10
11A YPR S	2.7	762	3.9	25.7					
12 NSS S	4.0		3	85.60	31	1.40			
13 BR3 S	4.4		2.9	79.7		1.25 ± .07	.23 ± .02	.070 ± .005	4.2 ± .3
14 BR3 S	4.4		3.9	84.7		1.25 ± .02	.19 ± .01	.060 ± .004	3.70 ± .25

* W/U is the ratio between the volume of water in a unit cell and the volume the uranium would occupy were it in the form of metal.

** These have been corrected to a cutoff of 0.625 ev from an assumed experimental Cd cutoff of 0.49 ev. The corresponding correction to ρ₂₈ is negligible.

† h = hexagonal lattice of fuel rods; S = square lattice.

TABLE 6

Physical Data of Experimental Lattices

Case	UO ₂ Density gm/cm ³	UO ₂ Pellet Diameter, cm	Clad I.D. cm	Clad Thickness cm	Lattice Pitch cm	Clad Material
1	7.530	1.524	1.5494	.0711	2.205	Al
2	"	"	"	"	2.359	Al
3	"	"	"	"	2.512	Al
4	7.516	.98298	1.0084	.0711	1.558	Al
5	"	"	"	"	1.652	Al
6	10.532	.98298	1.0084	.0711	1.558	Al
7	"	"	"	"	1.652	Al
8	"	"	"	"	1.806	Al
9 and 9A	10.179	.762	.7776	.08189	1.0287	Steel
10 and 10A	"	"	"	"	1.1049	Steel
11 and 11A	"	"	"	"	1.1938	Steel
12	9.636	1.1268			1.6841	Steel
13	9.910	.7592	.75920	.05334	1.1049	Steel
14	"	"	"	"	1.1938	Steel

TABLE 7

Homogenized Number Densities in Experimental Lattices

Case	Atomic Number Densities, Atoms per barn-cm									
	H	O	C*	B ¹⁰	Al	U-235	U-238	Fe	Cr	Ni
1	.03128	.03023	.0006411		.005188	.00009644	.007168			
2	.03577	.03063	.0005598		.004529	.00008420	.006259			
3	.03943	.03096	.0004939		.003997	.00007430	.005522			
4	.03382	.02910	.0005353		.006929	.00008053	.005985			
5	.03752	.02958	.0004752		.006150	.00007148	.005313			
6	.03385	.03350	.00001873		.006914	.0001102	.008192			
7	.03750	.03348	.00001665		.006146	.00009797	.007282			
8	.04226	.03347	.00001394		.005146	.00008203	.006097			
9	.030145	.034646				.00026718	.0095196	.0060611	.0016886	.0007834
9A	.029762	.033212		.2054x10 ⁻⁵	.0024816	.00025059	.0089152	.005556	.0015479	.0007181
10	.035018	.034476				.00023160	.0082518	.0052540	.0014638	.0006790
10A	.034437	.033102		.3956x10 ⁻⁵	.0024098	.00021713	.0077246	.0048178	.0013422	.0006227
11	.039567	.034317				.00019839	.0070686	.0045006	.0012539	.0005817
11A	.038797	.032997		.4632x10 ⁻⁵	.0023318	.00018589	.0066135	.0041212	.0011482	.0005326
12	.03734	.03362				.00029896	.007175	.0056442	.0014724	.0008998
13	.033997	.032344			.0026181 [†]	.00034250	.0073305	.0064498	.0018416	.0008838
14	.038420	.032350			.0025324 [†]	.00029325	.0062764	.0055224	.0015768	.0007094

* An impurity in the fuel pellets.

† Al followers on the control rod.

IV. COMPARISON BETWEEN EXPERIMENT AND THE SEMI-EMPIRICAL THEORY

The lattice parameters introduced in Section II above may be divided into two categories; those which are independent of the values of the fittable parameters a and b , and those which depend on them. It is convenient to consider the former category before discussing the search for the best fit to a and b .

1. Quantities which are independent of a and b .

This grouping includes $\bar{\phi}_3/\bar{\phi}_1$, ηf , L^2 , ϵ , δ_{28} , τ , p_{25} , η_{25}^R , and p_c . Table 8 is a listing of the calculated values of these quantities. Comparison of calculated and experimental values of $\bar{\phi}_3/\bar{\phi}_1$ and δ_{28} (Table 10) show excellent agreement in the flux ratios; the δ_{28} comparison might be termed "reasonable".

2. Fitting of a and b .

The important quantities which depend on a and b are ρ_{28} , p_{28}^U , δ_{25} , β , k_{eff} , and $\partial\rho/\partial B^2$. Calculations of these quantities were performed for values of $a = 0.5, 0.6,$ and 0.7 and $b = 0.7, 0.8,$ and 0.9 . Table 9 shows the values of k_{eff} calculated for the critical bucklings given in Table 5 for the various values of a and b chosen. Figure 3 is a contour plot illustrating the choice of a and b values which seem to provide a minimum of the quantity $\Sigma (k - 1)^2$.

Thus, having fitted the model to provide a best prediction to measured critical sizes, we finally have $a = 0.5$, $b = 0.86$. Table 10 presents values of k , $\partial\rho/\partial B^2$, ρ_{28} , and δ_{25} calculated on the basis of these values of a and b . It also recapitulates the calculated δ_{28} and $\bar{\phi}_3/\bar{\phi}_1$ values presented in Table 8, and reproduces the experimental data of Table 5. The agreement in k is good, that in the detailed lattice parameters is fair, except for the large disagreement among ρ_{28} values for the Yankee criticals.

TABLE 8

Hand Calculated Lattice Parameters Independent of a and b

Case	$\bar{\phi}_3 / \bar{\phi}_1$	η_f	L^2	ε	δ_{28}	τ	P_{28}	P_{25}	η_{25}^R	P_c
1	1.1368	1.3713	4.4658	1.0539	.0719	51.76	.8017	.9537	1.700	.9879
2	1.1477	1.3209	4.2953	1.0440	.0588	48.18	.8413	.9640	1.698	.98886
3	1.1581	1.2708	4.2445	1.0368	.0497	45.40	.8690	.9708	1.696	.9893
4	1.0868	1.3233	4.6860	1.0438	.0592	52.08	.8177	.9636	1.698	.9882
5	1.0909	1.2772	4.5620	1.0368	.0500	48.77	.8486	.9705	1.696	.9888
6	1.1245	1.3783	3.6888	1.0560	.0750	42.51	.7879	.9514	1.702	.9876
7	1.1300	1.3408	3.6286	1.0476	.0636	40.78	.8223	.9604	1.699	.9884
8	1.1389	1.2787	3.6496	1.0377	.0508	38.80	.8620	.9700	1.696	.9891
9	1.1601	1.5105	2.1099	1.0660	.0870	38.67	.7203	.8814	1.716	.9549
10	1.1668	1.4875	2.0680	1.0541	.0698	37.14	.7746	.9082	1.712	.9639
11	1.1749	1.45866	2.0826	1.0441	.0561	35.93	.8190	.9282	1.708	.9704
12	1.3646	1.5518	1.7685	1.0461	.0558	36.87	.8253	.8914	1.716	.9623
13	1.2561	1.6006	1.7356	1.0492	.0600	38.95	.7880	.8678	1.721	.9580
14	1.2713	1.5754	1.7720	1.0400	.0482	37.62	.8316	.8959	1.716	.9658

TABLE 9

Fit of k (using B_{crit}^2) as a Function of a and b^*

CASE	a	.5			.6			.7		
	b	.7	.8	.9	.7	.8	.9	.7	.8	.9
1		1.0078	1.0068	1.0060	1.0063	1.0053	1.0044	1.0047	1.0038	1.0029
2		1.0066	1.0060	1.0052	1.0057	1.0050	1.0043	1.0048	1.0040	1.0034
3		1.0037	1.0031	1.0026	1.0030	1.0025	1.0020	1.0024	1.0019	1.0013
4		.9924	.9917	.9910	.9912	.9906	.9899	.9901	.9896	.9889
5		.9931	.9926	.9921	.9924	.9919	.9914	.9917	.9912	.9907
6		1.0047	1.0038	1.0028	1.0028	1.0019	1.0010	1.0012	1.0002	.9994
7		1.0029	1.0021	1.0013	1.0017	1.0009	1.0001	1.0005	.9997	.9990
8		1.0010	1.0004	.9998	1.0002	.9997	.9991	.9996	.9990	.9985
9		1.0023	.9995	.9968	.9959	.9932	.9907	.9898	.9873	.9849
10		1.0070	1.0045	1.0021	1.0034	1.0008	.9985	.9998	.9974	.9952
11		1.0038	1.0017	.9997	1.0016	.9996	.9975	.9995	.9974	.9955
12		1.0065	1.0022	.9982	1.0032	.9992	.9952	1.0001	.9961	.9922
13		1.0070	1.0018	.9969	1.0021	.9971	.9923	.9972	.9923	.9877
14		1.0053	1.0010	.9971	1.0024	.9982	.9944	.9995	.9955	.9912
$\Sigma (k-1)^2$		4.430×10^{-4}	2.670×10^{-4}	2.588×10^{-4}	2.785×10^{-4}	2.772×10^{-4}	4.238×10^{-4}	3.321×10^{-4}	4.903×10^{-4}	7.958×10^{-4}

* Lattices 9A, 10A, and 11A were ignored in making the fit of a and b .

TABLE 10

Comparison of Experiment with Semi-Empirical Model

Case	Calc.* k_{eff}	$\bar{\rho}_3/\bar{\rho}_1$		δ_{28}		δ_{25}		ρ_{28}		$\partial\rho/\partial B^2$	
		Exp.	Calc.	Exp.	Calc.	Exp.	Calc.	Exp.	Calc.	Exp.	Calc.
1	1.0062	1.09 \pm .03	1.137	.071 \pm .010	.0719	.075 \pm .003 - .008	.0705	1.19 \pm .04	1.321	48 \pm 2	52.3
2	1.0055	1.14 \pm .03	1.148	.059 \pm .009	.0588	.072 \pm .002 - .010	.0549	.99 \pm .013	1.043	46 \pm 2	48.3
3	1.0028	1.16 \pm .03	1.158	.051 \pm .004	.0497	.067 \pm .002 - .010	.0449	.807 \pm .014	.860	41 \pm 2	45.9
4	.9913	1.10 \pm .01	1.087	.063 \pm .003	.0592	.073 \pm .002 - .010	.0553	1.04 \pm .05	1.211	47 \pm 2	52.9
5	.9923	1.10 \pm .01	1.091	.054 \pm .003	.0500	.053 \pm .002 - .009	.0451	.90 \pm .02	1.001	48 \pm 2	49.7
6	1.0032	1.10 \pm .01	1.124	.078 \pm .004	.0750	.083 \pm .002	.0744	1.43 \pm .01	1.439	41 \pm 2	43.4
7	1.0016	1.13 \pm .01	1.130	.070 \pm .004	.0636	.067 \pm .001	.0603	1.15 \pm .01	1.181	39 \pm 2	41.1
8	1.000	1.13 \pm .01	1.139	.057 \pm .003	.0508	.052 \pm .001	.0460	.93 \pm .01	.912	36 \pm 2	39.2
9	.9979	---	1.160	---	.0870	---	.194	2.77 \pm .08	4.13	38 - 43	41.1
9A	1.0060	---	1.160	---	.0853	---	.192	---	4.07	---	45.0
10	1.0031	1.16 \pm .05	1.167	.076 \pm .002	.0698	.15 \pm .01	.142	2.22 \pm .05	3.12	37 - 38	36.9
10A	1.0081	---	1.168	---	.0704	---	.148	---	3.21	---	41.7
11	1.0004	1.16 \pm .03	1.175	.060 \pm .005	.0561	---	.107	1.85 \pm .10	2.39	32 - 36	34.6
11A	1.0065	---	1.176	---	.0579	---	.115	---	2.54	---	40.1
12	.9999	1.40	1.365	---	.0558	---	.162	---	3.30	31	33.8
13	.9944	1.25 \pm .07	1.256	.070 \pm .005	.0600	.23 \pm .01	.202	4.2 \pm .3	4.61	---	36.9
14	1.0159	1.25 \pm .02	1.271	.060 \pm .004	.0482	.19 \pm .01	.151	3.70 \pm .25	3.47	---	33.7

* a = .5

b = .86

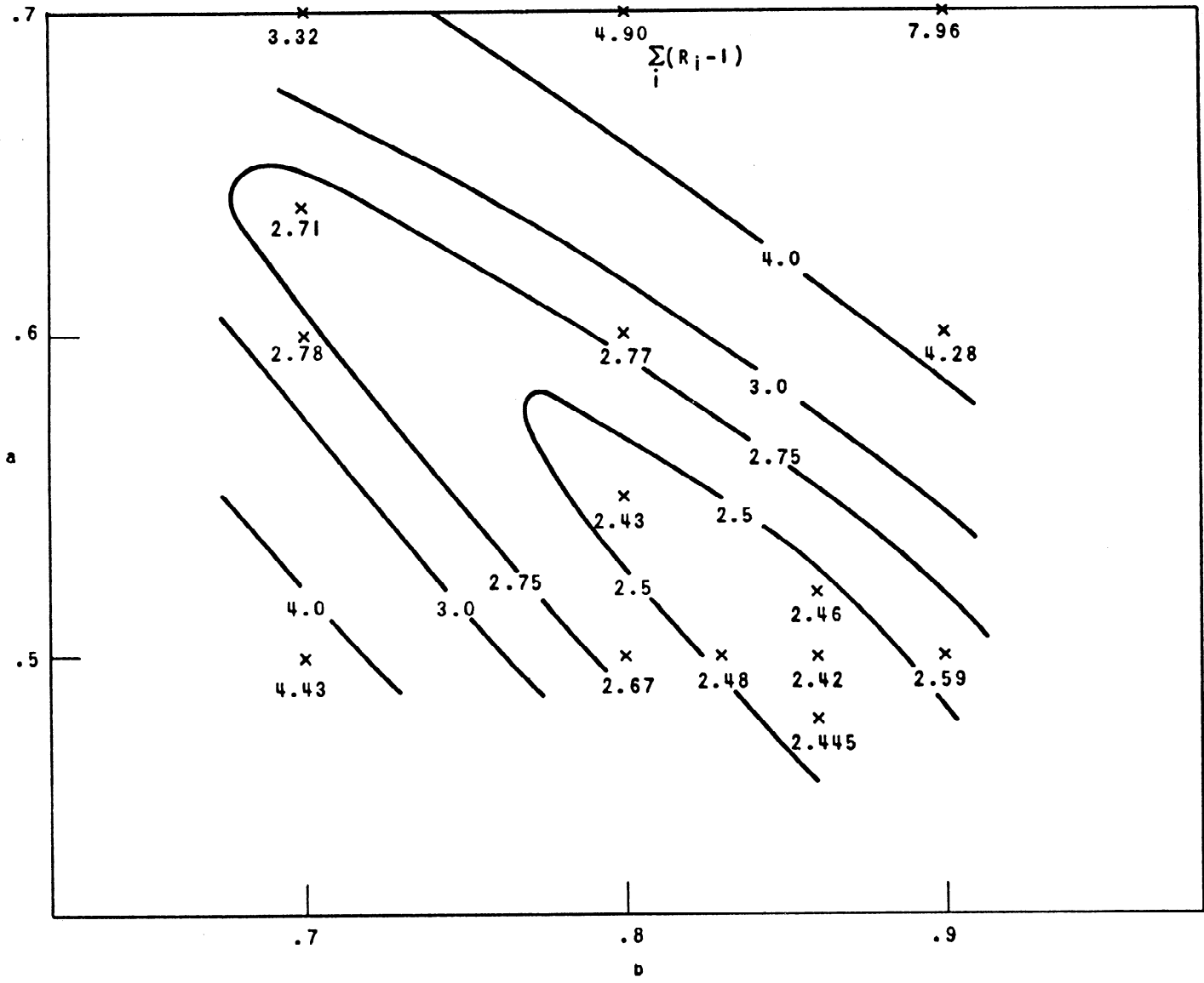


FIGURE 3
CONTOUR PLOT TO DETERMINE BEST FIT OF a AND b

V. A SYSTEM INVOLVING THE MUFT CODE AND ITS COMPARISON WITH EXPERIMENT

As described in Section I, the microscopic approach would give the nuclear designer more confidence in extrapolations beyond the range of experimental data. Although the methods necessary for a completely microscopic calculation are not presently available, this section describes an attempt to at least move in the direction of less empiricism. The method presented here may prove valuable in the design of future cores.

The MUFT code⁶ would seem at first glance to provide an ideal solution to the problem of treating the simultaneous leakage and resonance capture of intermediate energy neutrons. This code (coupled with the same SOFOCATE thermal constants mentioned above in Section III 2) provides 55 energy groups of neutrons and what would seem to be adequate orders of approximation in angular distributions (P-1) and slowing down (the Greuling-Goertzel-Amster scheme: exact for hydrogen, better than age theory for other elements¹¹) in this range of reactor sizes. There are two problems, however, which make even MUFT less than adequate at face value.

In the first place the 54 groups of fast neutrons do not provide a fine enough energy structure to sort out adequately the resonances of U-235 and U-238. When five or six resonances fall in a single group they become hopelessly jumbled and one cannot expect the code to calculate properly the rate of capture in each resonance. It would be possible to modify the code library to use a larger number of groups, but some of the U-235 and U-238 resonances actually overlap.

The second problem which arises is that of heterogeneity. The MUFT code assumes a homogeneous mixture, but a self shielding factor L can be supplied as input to alter the resonance capture rate in each resonance to account for heterogeneity. Presumably the proper choice of

an L factor for each resonance would yield good results from the MUFT model*. One way to obtain such a set of L factors would be from a Monte Carlo calculation in which the capture rates were calculated for each resonance separately and sorted by element. No such code exists at present.

The approach that has been taken is to calculate the rate of U-238 resonance captures from the semi-empirical model (see equation 13) and require MUFT to search for the L factor (assumed the same for all U-238 resonances) necessary to equal this rate**. In view of the low enrichments of all of these experiments, it was felt to be sufficient to use an L of 1 for all U-235 resonances, although perhaps it would have been better to use a smaller factor to account for the shielding effect of U-238 resonances. (If such a number could be calculated.)

Table 11 shows the results of the application of this modified MUFT, where the ρ_{28} values of Table 10 (and SOFOCATE values of f_{28}) were used as input. In general, the results seem to be quite good, although the δ_{25} values seem high, indicating the use of $L_{25} < 1$ or an error in the library constants. (This MUFT library contains the 25 resonance parameters explicitly.)

* By the "MUFT model" is meant that one calculates k_2 from the formula in Appendix A, using the MUFT and SOFOCATE 2 group constants and the measured critical B^2 .

** See Appendix E for a more precise description of this process.

TABLE 11

Use of MUFT Code in Comparison with Experiment

Case	MUFT k_2^*	δ_{28}		δ_{25}		$\partial\rho/\partial B^2$	
		Exp.	MUFT	Exp.	MUFT	Exp.	MUFT
1	.9980	.071 \pm .010	.0737	.075 \pm .003 - .008	.0931	48 \pm 2	48
2	1.0012	.059 \pm .009	.0608	.072 \pm .002 - .010	.0726	46 \pm 2	44
3	1.0017	.051 \pm .004	.0518	.067 \pm .002 - .010	.0597	41 \pm 2	42
4	.9892	.063 \pm .003	.0610	.073 \pm .002 - .010	.0742	47 \pm 2	47
5	.9922	.054 \pm .003	.0520	.059 \pm .002 - .009	.0609	48 \pm 2	44
6	.9946	.078 \pm .004	.0768	.083 \pm .002	.0986	41 \pm 2	40
7	.9968	.070 \pm .004	.0656	.067 \pm .001	.0802	39 \pm 2	37
8	.9982	.057 \pm .003	.0529	.052 \pm .001	.0614	36 \pm 2	36
9	.9905	---	.0874	---	.263	38 - 43	35
9A	1.0027	---	.0858	---	.258	---	-
10	.9940	.076 \pm .002	.0707	.15 \pm .01	.193	37 - 38	33
10A	1.0078	---	.0718	---	.199	---	-
11	.9942	.060 \pm .005	.0572	---	.145	32 - 36	31
11A	1.0086	---	.0595	---	.154	---	-
12	.9865	---	.0563	---	.222	31	30
13**	.9947	.070 \pm .005	.0639	.23 \pm .01	.299	---	-
14**	.9961	.060 \pm .004	.0524	.19 \pm .01	.221	---	-

* See Appendix A.

** These were run on PDQ because the core had Al followers on the control rods.

APPENDIX A

GROUP CONSTANTS AND k_{eff}

The group constant scheme adopted here is the one used in the Bettis diffusion codes (WANDA¹², PDQ¹³, etc.). It appears as follows in the four group version: (Cuts at .821 Mev, 5.53 kev, and 0.625 ev.)

$$(D_1 \nabla^2 - \Sigma_{a1} - \Sigma_{r1}) \phi_1 + \chi_1 \left(\frac{\nu \Sigma_{1f} \phi_1 + \nu \Sigma_{2f} \phi_2 + \nu \Sigma_{3f} \phi_3 + \nu \Sigma_{4f} \phi_4}{\lambda} \right) = 0 \quad (\text{A1})$$

$$(D_2 \nabla^2 - \Sigma_{a2} - \Sigma_{r2}) \phi_2 + \Sigma_{r1} \phi_1 + \chi_2 \left(\frac{\nu \Sigma_{1f} \phi_1 + \nu \Sigma_{2f} \phi_2 + \nu \Sigma_{3f} \phi_3 + \nu \Sigma_{4f} \phi_4}{\lambda} \right) = 0 \quad (\text{A2})$$

$$(D_3 \nabla^2 - \Sigma_{a3} - \Sigma_{r3}) \phi_3 + \Sigma_{r2} \phi_2 = 0 \quad (\text{A3})$$

$$(D_4 \nabla^2 - \Sigma_{a4} - \Sigma_{r4}) \phi_4 + \Sigma_{r3} \phi_3 = 0 \quad (\text{A4})$$

λ in these formulas is generally called the eigenvalue, and has many of the properties of a k . It is a measure of the reduction in ν necessary to achieve criticality with the given set of group constants. It has been called k in the remainder of this report. Note that $\Sigma_{r4} = 0$.

A hand solution of these equations is possible when the geometry is sufficiently simple that $\nabla^2 \phi = -B^2 \phi$, and B^2 is constant. This will occur in a bare slab, cylinder or sphere. In this simple case, ϕ can be cancelled from all four equations, allowing us to solve for k :

$$k_4 = \frac{\chi_1 \nu \Sigma_{1f}}{A_1} + \frac{\nu \Sigma_{2f}}{A_2} \left(\chi_2 + \frac{\chi_1 \Sigma_{r1}}{A_1} \right) + \frac{\nu \Sigma_{3f}}{A_3} \left(\frac{\chi_1 \Sigma_{r1} \Sigma_{r2}}{A_1 A_2} + \frac{\chi_2 \Sigma_{r2}}{A_2} \right) + \frac{\nu \Sigma_{4f}}{A_4} \left(\frac{\chi_1 \Sigma_{r1} \Sigma_{r2} \Sigma_{r3}}{A_1 A_2 A_3} + \frac{\chi_2 \Sigma_{r2} \Sigma_{r3}}{A_2 A_3} \right) \quad (\text{A5})$$

$$A_i = D_i B^2 + \Sigma_{ri} + \Sigma_{ai} \quad (\text{A6})$$

The two group formula follows obviously from the above if $\chi_1 = 1$, $\chi_2 = 0$:

$$k_2 = \frac{v\Sigma_{1f}}{A_1} + \frac{v\Sigma_{2f} \Sigma_{1r}}{A_1 A_2} \quad (A7)$$

Of course none of the experiments were performed in bare reactors: all cases were measured in water-reflected cylinders. However, the measured critical B^2 values were obtained from fits of flux traverses over core central regions to $J_0(B_r r)$ and $\cos(B_z z)$ functions. They should thus correspond to bare cores of dimensions corresponding to B_r and B_z , i.e.; the actual dimensions increased by the reflector savings. The calculated MUFT-SOFOCATE k values presented in Table 11 of this report were obtained through the use of equation A7. Table A1 should quell any doubts about the use of this simple formula, as it shows the excellent agreement between k_2 and k_4 (equations A7 and A5) on the one hand, and the eigenvalues of two and four group two region WANDA's run for explicit representations of the core-reflector geometry.

Table A1 also shows some selected results obtained by running the PLMG code¹⁸. This is a 55 group diffusion code, and corresponds to a spatial MUFT, in which one does not assume a B^2 which is held constant over the core (separability of space and energy). The same library of constants is used in PLMG as in MUFT (except that PLMG employs the consistent Greuling-Goertzel approximation¹⁹), while the L factors used were taken from the core MUFT's which had converged to $\rho_{28} f_{28}$.

TABLE A1

Comparison Between k_2 , k_4 , and WANDA Eigenvalues

Case	Core [†] Radius cm	B_z^2 expt'l. [†] cm ⁻² x 10 ⁴	k_2^*	k_4^*	4 Group ^{**} WANDA	2 Group ^{**} WANDA	PLMG k
1	41.25	5.05	.9980	.9979	.9984	.9983	.9941
2	39.71	5.13	1.0012	1.0009	.9997	.9999	.9970
3	41.44	5.20	1.0017	1.0017	1.0008	1.0012	.9994
4	45.14	5.11	.9892	.9893	.9894	.9894	
5	45.80	5.24	.9922	.9920	.9919	.9923	
6	38.13	5.24	.9946	.9946	.9947	.9944	
7	36.34	5.29	.9968	.9968	.9970	.9970	
8	37.63	5.30	.9982	.9982	.9978	.9982	
9	32.01	5.42	.9905	.9905	.9882	.9876	
9A	41.13	5.42	1.0027	1.0026	.9988	.9987	
10	26.82	5.42	.9940	.9940	.9905	.9906	
10A	43.88	5.42	1.0078	1.0078	1.0036	1.0037	
11	24.27	5.42	.9942	.9942	.9924	.9931	
11A	46.03	5.42	1.0086	1.0088	1.0058	1.0060	
12	19.3	3.53	.9865	.9865	.9872	.9885	.9938
13	20.70	4.30	.9947		.9894	.9894	
14	19.13	4.10	.9961		.9918	.9940	

* k_2 and k_4 were calculated using the B_{crit}^2 values (from Table 5) in equations A7 and A5, respectively.

† These values were obtained from references 2, 10, and 17.

** These numbers are the eigenvalues of cylindrical two region WANDA's, in which a core of the radius in column 2 is surrounded by a 6" (∞) H₂O reflector. B_z^2 is fed in as the transverse buckling. The reflector constants were obtained from a pure H₂O MUFT and SOFOCAT. Cases 13 and 14 are two group PDQ's.

APPENDIX B

FAST FISSION CONSTANTS

Consider first δ_{28} , the ratio of U-238 fissions to U-235 fissions. This can be calculated easily from the four group model of equations A1 through A4, after the substitution $\nabla^2 \phi = -B^2 \phi$. If we assume a power normalization such that C is the number of neutrons from all fissions in groups 2, 3, and 4; then the group 1 equation (all U-238 fissions are in group 1) is as follows:

$$-A_1 \phi_1 + \chi_1 v \Sigma_{1f} \phi_1 + \chi_1 C = 0 \quad (A8)$$

$$v \Sigma_{1f} = v \Sigma_{1f28} + v \Sigma_{1f25} \quad (A9)$$

$$\phi_1 = \frac{\chi_1 C}{A_1 - \chi_1 v \Sigma_{1f}} \quad (A10)$$

Then the definition of δ_{28} can be expressed

$$\delta_{28} = \frac{\text{number 28 fissions}}{\text{number 25 fissions}} = \frac{\phi_1 v \Sigma_{1f28} / v_{28}}{\frac{C + v \Sigma_{1f25} \phi_1}{v_{25}}} \quad (A11)$$

$$\delta_{28} = \frac{v_{25}}{v_{28}} \left[\frac{\chi_1 v \Sigma_{1f28}}{A_1 - \chi_1 v \Sigma_{1f28}} \right] \quad \text{OK} \quad (A12)$$

However, ϵ has been defined in terms of a reactor in which there was neither leakage, radiative capture (n, γ), nor U-235 fissions in the first group. Let us define a fictitious $\bar{\delta}_{28}$ which applies in this case:

$$\bar{A}_1 = \Sigma_{1r} + \Sigma_{1f28} \quad (A13)$$

$$\bar{\delta}_{28} = \frac{\nu_{25}}{\nu_{28}} \left[\frac{\chi_1 \nu \Sigma_{1f28}}{\Sigma_{1r} - (\chi_1 \nu_{28} - 1) \Sigma_{1f28}} \right] \quad (A14)$$

ϵ follows directly from $\bar{\delta}_{28}$ if we consider the excess of neutrons formed by 28 fissions over those used in causing them:

$$\epsilon = 1 + \bar{\delta}_{28} \left(\frac{\nu_{28} - 1}{\nu_{25}} \right) \quad (A15)$$

$$= \frac{\Sigma_{1r} + (1 - \chi_1) \Sigma_{1f28}}{\Sigma_{1r} - (\chi_1 \nu_{28} - 1) \Sigma_{1f28}} \quad (A16)$$

APPENDIX C

U-238 RESONANCE CONSTANTS

In measuring resonance capture by U-238 in reactor lattices, one obtains the cadmium ratio of a suitably shaped U-238 foil (see reference 2, p. 56 ff.). From this cadmium ratio (R), one easily derives ρ , the ratio of U-238 activations over the Cd cutoff to those below:

$$\rho_{28} = \frac{1}{R-1} \quad (A17)$$

The experimental numbers of Table 5 were obtained from equation A17, but have been corrected to a cutoff of 0.625 ev. Note that the cadmium ratio measurement will include in ρ_{28} those radiative captures competing with fast fissions, which explains their absence from the ϵ formula (A16).

The derivation of the theoretical expression for ρ_{28} (equation 13) follows from a consideration of Figure 1. Going back to the argument leading to equations 1 and 2 of Section II, and substituting into the definition of ρ_{28} :

$$\rho_{28} = \frac{(\cancel{\eta f} + x) \epsilon P_{NL1} \left[(1 - P_{28}^U) + P_{28}^U P_{25} (1 - P_{28}^L) \right]}{(\cancel{\eta f} + x) \epsilon P_{NL1} P_{28}^U P_{25} P_{28}^L P_c P_{NL2} R_f P_{NL3} R_s f_{28}} \quad (A18)$$

R_s and R_f can be eliminated through the observation that their product should have a value sufficient to make $k_{eff} = 1$. Going back to equation 3, this means:

$$R_s R_f = \frac{1}{P_{NL1} P_{NL2} P_{NL3} \eta f \epsilon P_c P_{28}^U P_{28}^L \beta} \quad (A19)$$

Thus equation A18 becomes:

$$\rho_{28} = P_{NL1} \epsilon \frac{\eta f}{f_{28}} \frac{\beta}{P_{25}} \left[1 - P_{28}^U + P_{28}^U P_{25} - P_{25} P_{28} \right] \quad (A20)$$

APPENDIX D

U-235 RESONANCE CONSTANTS

Recent measurements of the U-235 resonance parameters^{14,15} were used to construct Figure 2. Table A2 gives the energies and parameters of the resonance included, as well as the assumed $1/v$ term. The resonance integral was calculated from the standard formula¹⁶:

$$RI_{25} = \int (\sigma_a)_{\text{eff}}^{25} \frac{dE}{E} = \int \frac{\sigma_{a25}}{1 + \frac{N_{25} \sigma_{a25}}{\Sigma_s}} \frac{dE}{E} \quad (\text{A21})$$

If we write σ_{a25} as a $1/v$ term plus a sum of single level Breit-Wigner resonances the integral in A21 can be evaluated if one assumes $E^{1/2} = E_0^{1/2}$. One then has:

$$RI_{25} = \frac{1}{v} \text{ term} + \frac{\pi}{2} \sum_{\text{resonances}} \frac{\frac{\sigma_{\text{amax}} (\Gamma_\gamma + \Gamma_f)}{E_0}}{\sqrt{1 + \frac{N_{25} \sigma_{\text{amax}}}{\Sigma_s}}} \quad (\text{A22})$$

The RI curve of Figure 2 is a plot of equation 22. The α curve is a plot of the ratio of an RI_γ to an RI_f ; where RI_γ is calculated from equation A22 with only Γ_γ and a capture $1/v$ term while RI_f is calculated using only Γ_γ and a fission $1/v$ term.

TABLE A2

U-235 Resonance Parameters

Energy of Resonance E_0 , ev	Capture Width Γ_γ , ev	Fission Width Γ_f , ev
$\frac{1}{v}$ term, infinite dilution	33 barns	122 barns
1.13	0.034	0.107
2.04	0.030	0.012
2.82	0.030	0.070
3.14	0.030	0.115
3.61	0.030	0.045
4.84	0.030	0.004
6.40	0.030	0.018
7.10	0.030	0.021
8.82	0.030	0.059
11.7	0.030	0.007
12.4	0.030	0.020
16.2	0.030	0.012
19.3	0.030	0.080
21.2	0.030	0.090
23.7	0.030	0.105
34.7	0.030	0.048
35.3	0.030	0.082

APPENDIX E

MODIFICATION OF MUFT CODE

MUFT was modified so that it would make an L factor search to force Σ_{c28}/Σ_r (one fast group) to agree with an input constant ω . Thus L for U-238 (or any other element for which such a search is desired) is no longer an input constant.

$\omega = \left(\frac{\Sigma_{c28}}{\Sigma_r} \right)$ is thus the ratio of neutrons captured by U-238 above 0.625 ev to those thermalized*. According to the loop model of Figure 1, this becomes (y is the number of neutrons getting by P_{NL1}):

$$\omega = \frac{y (1 - p_{28}^U) + y p_{28}^U p_{25} (1 - p_{28}^L)}{y p_{28} p_{25} p_c p_{NL2}} \quad (A23)$$

$$= \frac{1}{p_{28} p_{25} p_c p_{NL2}} \left[(1 - p_{28}^U) + p_{28}^U p_{25} - p_{28} p_{25} \right] \quad (A24)$$

$$= \rho_{28} f_{28} R_s R_f p_{NL3} \quad (A25)$$

To see the connection with conversion ratio (C.R.), consider the following:

$$\text{C.R.} = \frac{\text{rate of radiative captures in U-238}}{\text{rate of total captures in U-235}} \quad (A26)$$

$$= \frac{\left[\omega + R_f R_s p_{NL3} f_{28} \right] \Sigma_r \phi_f}{\left[\delta_{25} \frac{\nu_{25}}{\eta_{R25}} + \frac{\nu_{25}}{\eta_{25}} \right] f_{25} R_s R_f p_{NL3} \Sigma_r \phi_f} \quad (A27)$$

$$= \left(\frac{\eta_{25}}{\nu_{25}} \right) \left(\frac{f_{28}}{f_{25}} \right) \frac{1 + \rho_{28}}{1 + \delta_{25} \frac{\eta_{25}}{\eta_{R25}}} \quad (A28)$$

* Actually $\Sigma_r \phi_{fast}$ is not just the source of thermal neutrons - it also includes those neutrons captured above 0.625 by control material (unless such control material is specifically included in MUFT). R_f is thus left out of A23.

REFERENCES

1. W. H. Arnold, Jr., "Physics Calculations for Control Rods in the First Yankee Core," YAEC-62 (1959).
2. P. W. Davison, S. S. Berg, W. H. Bergmann, D. F. Hanlen, B. Jennings, R. D. Leamer, J. E. Howard, "Yankee Critical Experiments," YAEC-94 (1959).
3. A. Amouyal and P. Benoist, J. Nucl. En. 6, 79 (1957).
4. "Reactor Physics Constants," ANL-5800 (1958).
5. H. Amster, R. Suarez, "The Calculation of Thermal Constants Averaged Over a Wigner-Wilkins Flux Spectrum; Description of the SOFOCATE Code," WAPD-TM-39, (1957).
6. H. Bohl, Jr., E. Gelbard, G. Ryan, "Fast Neutron Spectrum Code for the IBM-704," WAPD-TM-72, (1957).
7. E. Hellstrand, J. Appl. Phys. 28, 1493, (1957).
8. S. M. Dancoff and M. Ginsburg, "Surface Resonance Absorption in a Close-Packed Lattice," CP-2157 (1944).
9. R. J. French, "The Dancoff Correction to Surface Absorption in Close-Packed Cylindrical Fuel Rod Lattices," YAEC-149, to be published in 1960.
10. H. Kouts, R. Sher, J. Brown, D. Klein, S. Stein, R. Hellens, W. H. Arnold, Jr., R. Ball, P. W. Davison, "Physics of Slightly Enriched, Normal Water Lattices (Theory and Experiment)," PICG 1958, P/1841.
11. W. H. Arnold, Jr., Nuclear Science and Engineering, 6, p. 456 (1959).
12. O. Marlowe, C. Saalbach, L. Culpepper, D. McCarty, "WANDA - A One-Dimensional Few Group Diffusion Equation Code for the IBM-704," WAPD-TM-28 (1956).
13. G. Bilodeau, W. Cadwell, J. Dorsey, J. Fairey, R. Varga, "PDQ - An IBM-704 Code to Solve the Two-Dimensional Few-Group Neutron Diffusion Equations," WAPD-TM-70, (1957).
14. O. D. Simpson, R. G. Fluharty, F. B. Simpson, Phys. Rev. 103, 971 (1956).
15. V. E. Pilcher, J. A. Harvey, D. J. Hughes, Phys. Rev. 103, 1342 (1956).

REFERENCES CONT'D

16. A. M. Weinberg and E. P. Wigner, "The Physical Theory of Neutron Chain Reactors," University of Chicago Press, (1958).
17. P. W. Davison, V. E. Grob, D. F. Hanlen, R. D. Leamer, H. Ritz, and E. Santandrea; "Two Region Critical Experiments with Water Moderated Slightly Enriched UO₂ Lattices," YAEC-142 (1959).
18. H. Bohl, Jr., E. M. Gelbard, G. H. Ryan, and P. J. Fike, "PLMG - A One-Dimensional Multigroup Pl Code for the IBM-704," WAPD-TM-135, (1958).
19. G. Goertzel and E. Greuling, Nuclear Science and Engineering 7, p. 69 (1960).

ACKNOWLEDGEMENTS

The author would like to express his thanks particularly to:
R. J. French, for his help in discussions of the reactivity model;
R. E. Radcliffe, who spent many months performing the calculations;
and P. W. Davison and his staff, who were very helpful in providing
data from the Yankee and Two-Region criticals. G. H. Minton,
R. Dannels, and R. Cummings were helpful in modifying the MUFT code.
The reader should have become aware, well before reaching this point,
of the excellent job of typing done by Miss Shirley Buzzard.